CONTACT FATIGUE IN TURBINE ENGINES DUE TO AEROELASTIC AND INERTIAL LOADING

J.R. Calcaterra[1] and S. Naboulsi[2]
1. Materials and Manufacturing Directorate, Air Force Research Laboratory, Wright-Patterson AFB, OH 45433, USA
2. Rhamm Technologies, Dayton, OH 45440, USA

ABSTRACT

The following study examines the durability of contact areas on turbine blades and turbine disks in modern jet engines. Two separate sets of blade and disk geometries were analyzed. First, a standard finite element analysis was used to determine the influence of inertial loading on the disk from the blades. However, it is very difficult to resolve contact stresses accurately using state of the art finite element codes. Because of this, the stresses at the blade/disk interface were integrated over two-dimensional slices of the component. The resulting contact loads were input into a singular integral equation in order to solve for the stresses at the edge of contact. The resulting stresses were analyzed using several methods to account for R-value dependencies, such as the Smith-Watson-Topper parameter, in order to predict fatigue lives and life limiting locations on the blade/disk interface. Next, an aeroelastic analysis was conducted on the blade using rigidly fixed conditions along the contact surface. The blade displacements were recorded and used to perform a second contact analysis. Fatigue lives and life limiting locations were again predicted using the resulting stresses. The relative importance of aeroelastic and inertial loading on contact fatigue was then determined. Finally the results of the analysis were compared to damage found on actual components. It was found that for different engine designs in the same thrust class, the amount of inertial loading can differ by an order of magnitude while the aeroelastic loading can vary by a factor of five. Each of these has a significant affect on contact damage and fatigue lives. The differences in component stress state correlate well with the amount of damage and damage location typically seen during maintenance cycles. This result was independent of the fatigue parameters used to in the analysis. This study is the first one that compares contact damage analyses on two different components using both inertial and aeroelastic analysis. The results from this study will help guide future turbine engine designs.

1 INTRODUCTION

One damage mechanism that has an affect on all turbine engines is wear. Wear damage can take the form of standard wear, galling or fretting. Each of these wear types, when severe enough, can necessitate the early retirement of turbine engine components. The various forms of wear damage cause enough early retirement that the USAF has conducted a significant amount of research over the past 5 years dedicated to wear mitigation. A significant result of this research has been, in part, the development and implementation of a computer code based on Singular Integral Equations (SIE) that has enabled the accurate and rapid determination of contact stress in turbine engine components [1-2].

The following study applies singular integral equation analysis to predict the contact fatigue lives of two similar engine components. These components are two separate compressor disk spools. The spools bear a number of similarities. They are both made of titanium. They are used in the two different engines with the same form, fit and function. They have approximately the same scheduled maintenance. They are both the first two stages of the compressor, fourth and fifth total stages of the engine. Both engines have 13 total stages. These engines fly on the same aircraft and perform the same mission. Despite these similarities, one component is nearly always retired early due to wear damage while the other is retired only rarely. There are some significant differences in design specifics. Among these are differences in dovetail slot geometry (the area

where the blade attaches to the disk), the number of total blades on each disk and the relative tolerance specifications of the spools. The following study examines the differences in contact stresses for each of these two components. The differences in contact stresses are related to differences in predicted fatigue lives. This comparison is supported by stress analysis on an experimental dovetail fixture [3].

2 EXPERIMENTAL AND ANALYTICAL DETAILS

All experiments were performed on 10.2 mm (0.4-in) thick dovetail specimens made of Ti-6Al-4V. This particular Ti-6Al-4V material has been used in many similar studies [4-7]. The cyclic properties are a modulus of 116 GPa, yield strength of 930 MPa and ultimate strength of 970 MPa [4]. Dovetail experiments were performed on a 100 kN (22 kip) servo-hydraulic load frame with a collet grip on the hydraulic ram. The crosshead grip was the dovetail fixture shown in Figure 1.

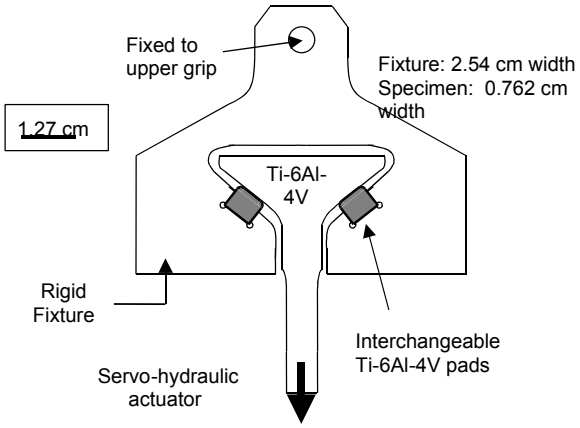

Figure 1: Schematic of dovetail gripping apparatus

The contact pads used in this study were cylindrical with a 52.8mm (2-in) radius. Due to the nature of contact fatigue, little instrumentation was used to characterize the test *in situ*. Experimental characterization is completed after failure using a Scanning Electron Microscope.
ANSYS was used to perform the analysis of both the dovetail specimens and the individual components. For the dovetail specimen, a two dimensional analysis was completed. An elastic material model was used to represent the Ti-6Al-4V material and no thermal effects were included. Eight-node, plane elements with a thickness function were used to represent the overall geometry of the dovetail specimen. Based on experimental measurements, the coefficient of friction (μ) was assumed to be 0.5.

The initial component finite element analysis was performed in a similar manner. Only elastic material response was modeled, no thermal effects were included and a coefficient of friction of 0.5 was assumed in order to arrive at the final stress state. However, these analyses were necessarily three dimensional because of the complex geometry of the components. The models were also much larger than the dovetail specimens and eight-node brick or eight-node tetrahedral elements were used to generate the structure of the model. For the initial analysis the stress range used for the life prediction parameter is based on the change in bulk stress of the blade bearing

against the disk from idle speed to the speed for sea level take off. In the case of these components, idle speed is approximately 1500 rpm and take off speed is 15,000 rpm. The difference between the initial and final analyses was that the final analysis included vibratory loading, as well as steady and unsteady aerodynamic driving forces. Finite element meshes for the two separate components are found in Figures 2 and 3. For simplicity, the first component will be referred to as component A and the second will be component B.

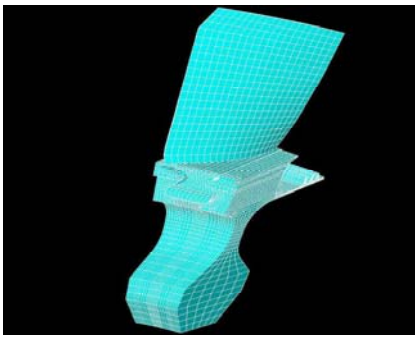

Figure 2: Finite element mesh for component A.

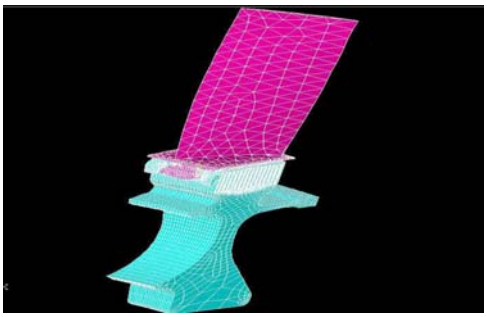

Figure 3: Finite element mesh for component B.

The geometries show in Figures 2 and 3 have been altered in order to prevent disclosure of design specifics. Because of this consideration, exact scales are not included. However, the reader can gain insight into the approximate design dimensions by using a height of 75 mm for the blade in component A and 100 mm for the blade in component B.

The finite element analysis used in this study to determine the contact stress is not sufficient to predict accurately the stresses at the edge of contact. Because of this, contact loads from the finite element analysis were used as input into a contact analysis program based on the SIE method. However, the SIE method is based on the assumption of elastic, two-dimensional contact. Since the turbine engine components are inherently three-dimensional, a hybrid process was used to perform the full contact analysis. The hybrid method breaks down a complex three-dimensional geometry into a series of two-dimensional approximations by slicing the finite element model

along node lines under the contact surface. Each of these slices is solved as a two-dimensional problem and then interpolated to form a three-dimensional picture of the stress state.

After the stress analyses were completed for the specimens and the components, a calculation of two stress parameters were made for each case. The stress parameters were the Smith-Watson-Topper (SWT) [8] parameter, $\sqrt{(\Delta\sigma)\sigma_{max}}$ based on maximum normal stress and the Findlay parameter [9], $\Delta\tau xy + (k\sigma x_{max}, k\sigma y_{max})$, based primarily on the shear stress range.

Each parameter was calculated at across the contact area and at 0.254mm (0.01in) increments into the contact depth. In addition, the contact parameters were rotated to determine the critical plane of the stress parameter.

3 RESULTS AND DISCUSSION

Stress results from both the initial and final component analyses were used to determine contact loads for input into the SIE code. The SIE code was then used to determine the contact stresses on the component slices and the specimen contact surface, shown in Figure 4.

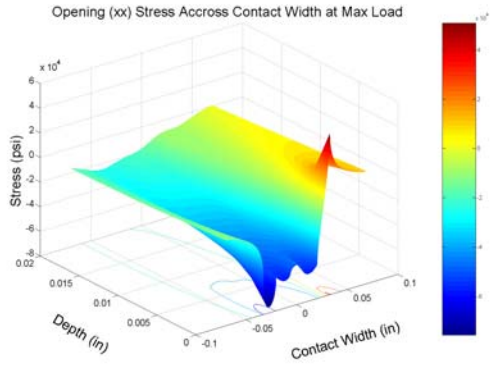

Figure 4: Opening stress, σxx, computed across a single contact slice.

After the stresses were computed for each contact slice, each stress parameter was calculated based on the contact stresses. This is shown in Figure 5.

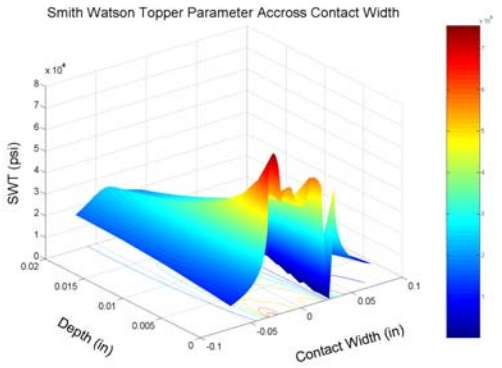

Figure 5: Computed SWT parameter for one slice on component B.

In order to determine the maximum value of each stress parameter on a component slice, the stresses were rotated. The parameter was then recalculated at one-degree intervals. This is shown in Figure 6.

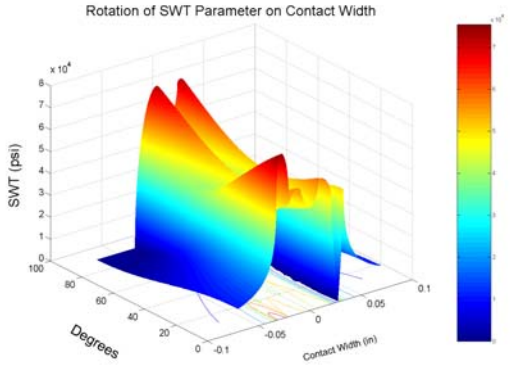

Figure 6: Rotation of the SWT parameter on one slice at the surface of component B.

Finally, each parameter on each component was interpolated at each depth to form a three-dimensional map of the stress variation in the contact zone. An example of this final interpolation is shown in Figure 7 for the contact surface.

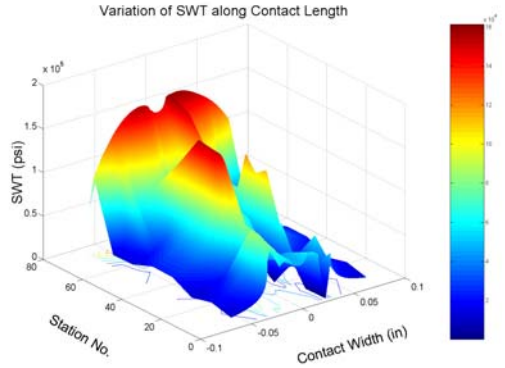

Figure 7: Interpolation of the SWT parameter on the dovetail slot of component B.

The maximum values of each stress parameter occurred at the contact surface. However, the stress parameters were typically higher on one side of the contact area. This correlates well to observed field damage. In addition, the maximum Findlay parameter typically occurred near a 45 degree rotation while the maximum SWT parameter typically occurred with no rotation.

4 CONCLUSIONS

Based on the proceeding study, the following conclusions can be drawn.

- There is a correlation between several critical plane parameters and the damage depth seen on both fielded hardware and laboratory specimens
- Differences in damage parameter evolution through the depth indicates critical distance techniques may not be consistent for general geometries

- Critical plane parameters based on maximum normal stress are predominantly highest on 0o plane and contact surface while maximum shear stress range parameters are highest between 40^o and 50^o.
- A qualitative comparison of the relative influences of inertial and aerodynamic loading indicate that the inertial loading causes the predominance of contact stresses. This relationship will be quantified during the presentation.

ACKNOWLEDGEMENT

All of this work was performed using funding provided by the Air Force Office of Scientific Research, project monitor Dr. Craig Hartley.

References

[1] McVeigh, P.A., Harish, G., Farris, T.N., and Szolwinski, M.P., "Modeling Interfacial Conditions in Nominally Flat Contacts for Application to Fretting Fatigue of Turbine Engine Components," *International Journal of Fatigue,* Vol. 21, (1999), pp. 5157-5165

[2] Ciavarella, M., "Indentation by Nominally Flat Indenters with Rounded Corners," *International Journal of Solids and Structures,* 36, (1999), pp. 4149-4181.

[3] Gallagher, J.P., *et al.,* "Improved High Cycle Fatigue (HCF) Life Prediction," *AFRL-ML-WP-TR-2001-4159*, (2001)

[4] Ritchie, R.O., Boyce, B.L., Campbell, J.P., and Roder, O., "High Cycle Fatigue of Turbine Engine Alloys," *Proceedings of the Fatigue Symposium*, The Society of Materials Science, Kyushu, Japan, (1998)

[5] Lanning, D.B., Haritos, G.K., and Nicholas, T., "Influence of Stress State on High Cycle Fatigue of Notched Ti-6Al-4V Specimens," *International Journal of Fatigue,* 21, (1999), pp. S87-S95.

[6] Ruschau, J.J., John, R., Thompson, S.B., and Nichaols, T., "Fatigue Crack Nucleation and Growth Rate Behavior of Laser Shock Peened Titanium," *International Journal of Fatigue,* 21, (1999), pp. S199-S209.

[7] Murthy, H., Farris, T.N., and Slavik, D.C., "Fretting Fatigue of Ti-6Al-4V Subjected to Blade/Disk Contact Loading," *Materials Science Research International Special Technical Publication: Materials Science for the 21st Century,* Osaka, Japan, (May 2001), pp. 200-207.

[8] Smith, K., Watson, P., and Topper, P., "A Stress Strain Function for the Fatigue of Metals," *Journal of Materials*, JMLSA, Vol. 5, No. 4, (1970), pp. 767-778

[9] Kallmeyer, A., Krgo, A., and Kurath, P., "Multiaxial Fatigue Life Prediction Methods for Notched Bars of Ti-6Al-4V," *Proceedings of the 2001 National High Cycle Fatigue Conference,* Jacksonville, Fl., (2001)